Earthquake Geotechnical Engineering for Protection and Development of Environment and Constructions – Silvestri & Moraci (Eds)
© 2019 Associazione Geotecnica Italiana, Rome, Italy, ISBN 978-0-367-14328-2

Comparison of two CPT based methods for liquefaction assessment for selected sites of the Emilia Romagna region

V. Fioravante
The University of Ferrara, Ferrara, Italy

D. Giretti
ISMGEO Srl., Seriate, Bergamo, Italy

L. Martelli
Seismic Surveys of the Emilia-Romagna Region, Italy

ABSTRACT: The paper presents the application of a method for the liquefaction assessment to a series of CPTUs carried out in several sites the Emilia-Romagna region interested by the 2012 Emilia seismic sequence. The method was specifically calibrated for a natural sand retrieved from a site in the region where extensive liquefaction occurred. The results are compared with a CPT- based liquefaction evaluation procedure from literature.

1 INTRODUCTION

In the months of May and June 2012, the Italian region between Emilia Romagna, Lombardia and Veneto (south-east Po river plane) was shaken by a series of earthquakes (the Emilia seismic sequence), of which the two main events are the May 20 and May 29 earthquakes, characterized by moment magnitude of M_w=6.1 and M_w=5.9, respectively (http://cnt.rm.ingv.it/events?). Both the two earthquakes caused liquefaction in various areas of the Emilia Romagna Region, whose surficial effects were sand-blow manifestations of marginal/moderate severity and lateral spreading. Particularly, the May 20 shake produced significant and severe lateral spreading manifestations in the localities of San Carlo and Mirabello, which are located about 15 km SE of the epicentre (Fioravante et al. 2013).

The sites where liquefaction occurred were generally characterized by surficial sandy deposits (depth lower than 10 m) originated in the last 500-1000 years by rivers of Apennine origin, currently extinguished or diverted. As an example, the sandy deposits which liquefied at San Carlo and Mirabello and caused extensive lateral spreading were formed by the fluvial activity of the Reno river in the years between 1450 and 1770, after which the river was diverted. Only in few cases the sandy layers which experienced liquefaction were deposited by the Po river.

After the May 20 and 29 earthquakes, many in situ geophysical and geotechnical investigations were carried out by the Seismic Surveys of the Emilia-Romagna Region in order to evaluate the current state of the subsoil at the sites where liquefaction occurred. A considerable part of the geotechnical tests was focused on the analysis of the mechanical behaviour of the sand affected by liquefaction at the site of San Carlo. The tests carried out on the San Carlo sand (SCS, which is a medium fine sand with an average non-plastic fine content of 12.5%) included laboratory cyclic undrained triaxial tests and centrifuge cone penetration tests. The laboratory experimentation allowed the calibration of a direct correlation between SCS cone and cyclic resistance (Giretti & Fioravante, 2017) in the frame of the critical state soil mechanics.

To test its applicability to unaged sandy deposits similar to those present at San Carlo, the calibrated method was applied to a series of CPTUs carried out in several site of the Emilia Romagna region interested by the 2012 seismic sequence. The same CPTU were analysed using the CPT based method of Boulanger and Idriss (2014). The sites were selected as follows:

- Site Type A, characterised by the presence of sandy layers with limited fine content, originated by Apennine rivers, where liquefaction occurred during the 2012 seismic sequence;
- Site Type B: presence of sandy layers with limited fine content, originated by Apennine rivers, where liquefaction phenomena were not observed;
- Site Type C: presence of sandy layers with limited fine content, originated by the Po river, where liquefaction occurred;
- Site Type D: presence of sandy layers with limited fine content, originated by the Po river, where liquefaction phenomena were not observed.

In the liquefaction assessment, reference was made to the seismic loading experienced by the sites during the 2012 earthquakes, i.e. to a maximum moment magnitude $M_w = 6.1$ (which corresponds to a number of equivalent cycles $N = 5$, according to the Idriss 1999 approach) and to the maximum accelerations measured or estimated at the test sites. This paper describes the results obtained. Figure 1 shows a map of the tested sites, together with the earthquakes epicentres and liquefaction manifestation. In Figure 2, cone resistance q_c profiles typical of the four different site types listed above are shown. The Figure highlight the difference between sandy deposits originated by Apennine rivers and by the Po river. The first ones are shallower and usually characterised by low q_c values, or low density. The second ones are deeper, thicker and denser.

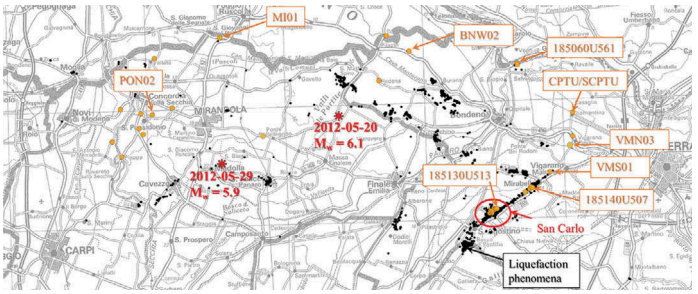

Figure 1. Map of the tested sites.

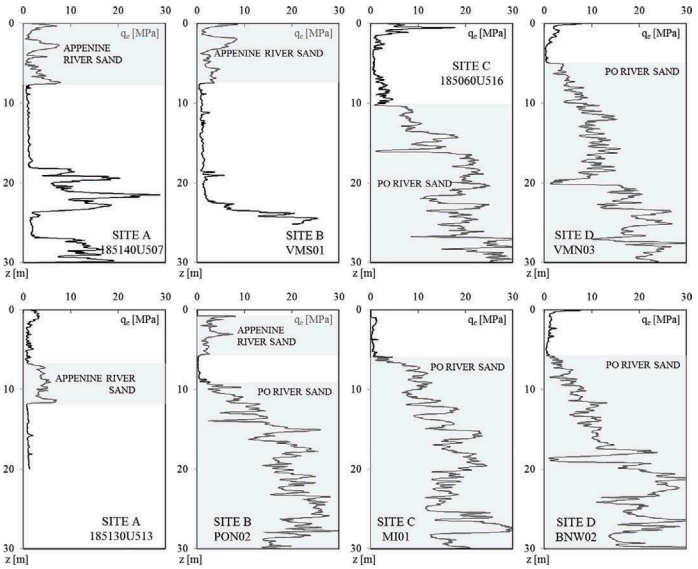

Figure 2. Typical cone resistance profiles.

2 THE METHOD ADOPTED

The method adopted for this study was originally developed on the base of the results of advanced laboratory tests available for two well-studied silica sands (Ticino and Toyoura, TS and TOS, Fioravante and Giretti 2016) and then extended to the natural sand retrieved at the site of San Carlo (SCS, Giretti and Fioravante 2017). The index properties and the grain size distribution of the sands are given in Table 1 and Figure 3. The following test results were interpreted: i) monotonic triaxial tests to define the sand critical state line in the e-p' and q-p' planes; ii) undrained cyclic triaxial tests to define the sand cyclic resistance; iii) centrifuge miniaturised cone penetration tests. The test interpretation was aimed at defining a direct correlation between the cone resistance q_c and the undrained cyclic resistance ratio CRR, using the state parameter ψ (Been & Jefferies, 1985) as linking variable. q_c and CRR of an uncemented and unaged soil depend on the material properties and the state of the soil, i.e. stress level and density. The latter two quantities can be expressed by the state parameter ψ, which is an indicator of the diection of volumetric strains (dilation or contraction) during shearing. This means that q_c and CRR are governed by the volumetric behaviour of the soil: the applied stress ratio to reach liquefaction at a defined number of cycles increases as ψ decreases; the penetration resistance of a soil is governed by the stress increment around the tip and the amount of the volumetric strains governs the stress variation respect to the initial level of stress.

Therefore, the direction and the amount of the volumetric strains can be expressed by the state parameter ψ which can be used to link directly CRR to the tip resistance of CPTs. In this context, the monotonic test results available for the reference sands were interpreted to define their critical state line and to associate at a given void ratio the relating state parameter. The test sands critical state parameters are listed in Table 2, in terms of Γ, λ and α, which are the material constants defining the position of the critical state line in the e – p' plane, according to Li & Wang, 1998:

$$e_{cs} = \Gamma - \lambda(p'/p_a)^{\alpha} \tag{1}$$

The shearing resistance angle at critical state, φ_{cs}, of TOS, TS and SCS is 31°, 34°, 34.7°, respectively.

The cyclic triaxial test results available were interpreted to define a correlation between the state parameter ψ and the applied cyclic stress ratio CSR at a given number of cycles N. The

Table 1. Index properties of the tested sands.

Sand	γ_{min} kN/m^3	γ_{max} kN/m^3	e_{min} -	e_{max} -	G_s -	D_{50} mm	U_c -
TOS	13.09	16.13	0.61	0.99	2.65	0.22	1.31
TS	13.64	16.67	0.57	0.92	2.68	0.53	1.3
SCS	13.37	16.95	0.55	0.96	2.67	0.21	-

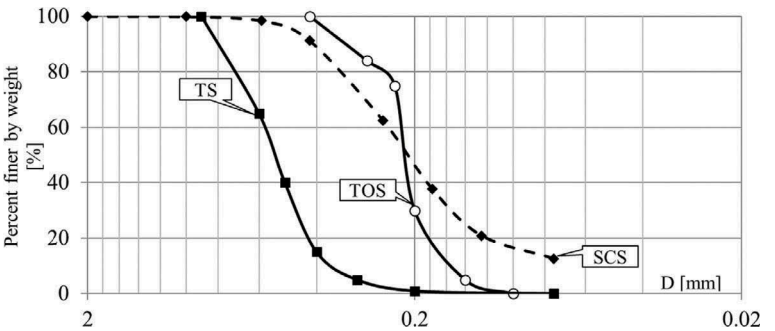

Figure 3. Grain size curves of the Ticino, Toyoura and San Carlo sands.

Table 2. Equations (1), (3), (4) and (5) fitting parameters.

	Eq. 1			Eq. 3			Eq. 4	Eq. 5	
Sand	Γ	λ	α	a	b	c	β	k	m
TOS	0.934	0.019	0.7	0.037	10.7	0.247	0.8	24	9.8
TS	0.923	0.046	0.5	0.071	7.8	0.177	0.8	28	8.1
SCS	0.99	0.12	0.59	0.115	3	0.145	1	27	7.4

cyclic undrained loading tests were interpreted assuming as failure condition the states at which the double amplitude axial strain $\varepsilon_a^{DA} = 5\%$. In the test interpretation, the applied cyclic stress ratio in triaxial condition, CSR^{TX}, was corrected into cyclic stress ratio for simple shear conditions (CSR^{SS}) via equation (Ishihara et al., 1977, 1985):

$$CSR^{SS} = CSR^{TX}(1 + 2k_0)/3 \tag{2}$$

where $k_0 = \sigma'_r/\sigma'_a$ = stress ratio at rest, computed as a function of the critical state shear resistance angle φ'_{cv} for normally consolidated samples using the equation of Jaky (1944).

The data analysed evidenced that the cyclic resistance of samples relating to a given ψ describeds clear relationships between CSR and N, whose slope in the semi-log plane was dependent on ψ. Those relationships were interpreted with a power function of N which accounts for the dependence of the cyclic resistance on ψ as follows:

$$CSR^{SS} = \frac{a(1-\psi)^b}{N^{c(1-\psi)}} \tag{3}$$

where a, b and c are empirical constants determined best fitting the available data and whose values are given in Table 2.

Equation 3 allows the estimation of the cyclic resistance ratio CRR^{SS} for any number of equivalent cycles; as an example for N = 15 the computed correlations for TS4, TOS and SCS are shown in Figure 4.

All the reference sands were subjected to centrifuge cone penetration tests carried out using the ISMGEO seismic centrifuge and miniaturized electrical piezocone. All the models were dry and homogeneous and were subjected to acceleration levels ranging from 30g to 100g. During the penetration in a homogeneous sandy soil the cone resistance experiences two opposite effects: (i) an increase in stress level due to the depth increase, which cause q_c to rise, and (ii) a decrease in the soil dilative tendency (in a homogeneous soil model ψ at rest increases as the depth increases, so the tendency of a soil to dilate reduces with depth) which imply a reduction of the rate of increase in q_c. To analyse the contribution of the overburden stress (p') and of the soil dilatancy (or state parameter ψ) on the measured cone resistance the following procedure was followed:

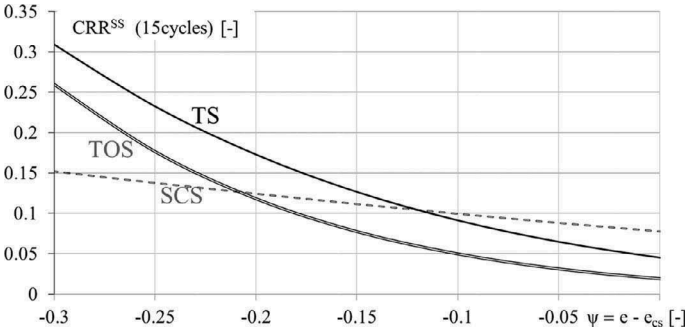

Figure 4. Cyclic resistance ratio at 15 cycles for simple shear conditions vs the state parameter ψ, for TS, TOS and SCS.

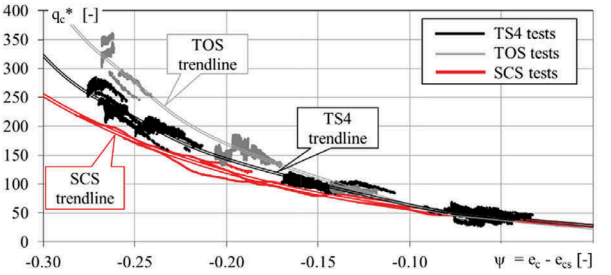

Figure 5. Normalized q_c^* vs. ψ for for TS, TOS and SCS.

- Effect of p': profiles of q_c characterized by constant ψ values were derived from the centrifuge CPTs. These q_c profiles were normalized by the reference atmospheric pressure (p_a= 101 kPa) and their dependence on the normalized overburden stress p'/p'_a analyzed. At constant ψ, q_c resulted a power law of p'. The following relation was derived:

$$q_c/p_a(p_a/p')^{\beta} = q_c* \tag{4}$$

The values of β given in Table 2 were found for the different sands analysed.

- Effect of ψ: the measured q_c profiles were normalized as per Eq. 4 and the q_c^* curves were plotted vs. ψ, as reported in Figure 5. The q_c^* - ψ trends were interpreted with the equation (adapted from Been et al., 1986):

$$q_c* = k \cdot e^{-m\psi} \tag{5}$$

where m and k are dimensionless fitting parameters, whose values are given in Table 2.

The data fitting curves are also plotted in Figure 5.

To evaluate CRR directly from q_c, Equations 3 and 5 were combined into Equation 6 to obtain a direct correlation between q_c^* and the cyclic resistance ratio at N cycles for simple shear condition, CRR_N^{SS}:

$$CRR_N^{SS} = \frac{a\left[1 + \frac{1}{m}\ln\left(\frac{q_c^*}{k}\right)\right]^b}{N^{c\left[1+\frac{1}{m}\ln\left(\frac{q_c^*}{k}\right)\right]}} \tag{6}$$

All the correlation parameters are listed in Table 2.

3 APPLICATION OF THE METHOD TO THE SELECTED TEST SITES

The 38 test sites selected for the application of method are listed in Table 3. In the table are also reported the following data: the ground water table (GWT) depth estimated at the sites on the base of the ground water model of the region, the maximum acceleration at ground surface registered or estimated at the sites during the 2012 seismic sequence, the depth of the sandy layer considered, the origin of the sandy layer (deposited by Apennine rivers or by the Po river), the occurrence of liquefaction manifestations during the 2012 earthquakes (which consisted in lateral spreading phenomena, marginal or moderate sand-blow manifestations elsewhere (severity of manifestations estimated according to Maurer et al. 2015), the site type (A, B, C or D). Of the 38 site, 14 are located at San Carlo and 4 at Mirabello. Of these, 17 out of 18 are cases of lateral spreading manifestations. Of the other 20 sites, 13 are type D, 3 type C and 1 type B. In 3 sites (PON02, POS01, POS03) are present both surficial Apennine river sands and deeper Po river sands.

For the application of Equation 6, a number of equivalent cycles N = 5 was considered, relating to an earthquake of moment magnitude M_w = 6.1, according to the Idriss 1999 approach. For the sites of types A and B the correlation parameters calibrated for SCS were

Table 3. Test sites and assessment parameters.

Locality	Test name	GWT (m)	a_{max} (g)	Layer depth from (m)	Layer depth To (m)	origin	liq	type	LPI I&B	LPI PS
San Carlo	185130U505	3	0.16	10	12.2	Ap	ls	A	0.87	0.78
	185130U506	3	0.16	8	12	Ap	ls	A	2.06	2.66
	185130U507	3	0.16	9.36	12	Ap	ls	A	1.16	1.77
	185130U508	3	0.16	8.7	11.5	Ap	ls	A	1.37	0.86
	185130U509	3	0.16	5	9.6	Ap	ls	A	2.11	2.18
	185130U510	3	0.16	10	12	Ap	ls	A	0.89	0.53
	185130U511	3	0.16	9.62	11.86	Ap	ls	A	0.88	2.06
	185130U512	3	0.16	10	12.3	Ap	ls	A	0.98	0.82
	185130U513*	3	0.16	6.78	11.7	Ap	ls	A	2.28	3.15
	185130U514	3	0.16	8.7	12.1	Ap	ls	A	1.37	1.95
	185130B501	3	0.16	8	10.8	Ap	ls	A	2.78	2.74
	185130B502	3	0.16	6	8	Ap	ls	A	0.34	1.35
	185130B503	3	0.16	9	12	Ap	ls	A	2.40	1.03
	185130B504	3	0.16	9.7	12.2	Ap	ls	A	2.01	0.93
Mirabello	185140U506	3	0.14	6	10.9	Ap	ls	A	1.20	1.09
	185140U507*	1	0.14	2	7.65	Ap	mo	A	6.80	6.13
	185140B502	3	0.14	8.25	12.4	Ap	ls	A	1.53	0.51
	185140B503	3	0.14	6	10	Ap	ls	A	0.89	1.33
Bondeno	185060U514	1	0.2	15	20	Po	ma	C	0.28	0.66
	185060U516*	1	0.2	10	20	Po	ma	C	4.54	3.83
	BNW01	1	0.28	12.5	20	Po	no	D	1.99	1.88
	BNW02*	1	0.28	6	18.2	Po	no	D	22.63	22.21
	BNW03	1	0.32	11	20	Po	no	D	8.68	9.13
Vigarano Mainarda	VMN01	1	0.12	8.8	20	Po	no	D	0.07	0.31
	VMN02	1	0.12	4.5	20	Po	no	D	0.27	0.36
	VMN03*	1	0.14	5.3	19.4	Po	no	D	2.43	2.09
	VMS01*	3	0.12	4	7.4	Ap	no	B	0.07	0.02
Concordia	COS01	1	0.32	14	20	Po	no	D	2.76	2.56
Secchia	COS05	1	0.32	12	20	Po	no	D	5.85	5.51
Mirandola	MI01*	1	0.3	6	20	Po	ma	C	15.19	12.69
San Felice sul Panaro	FPN02	1	0.32	10	20	Po	no	D	3.22	3.76
Novi di Modena	NMS01	1	0.25	11	20	Po	no	D	5.12	5.00
San Posidonio	PON01	1	0.32	13	20	PO	no	D	3.63	3.08
	PON02*	1	0.32	1	3.5	Ap	no	B	9.21	8.58
				9	20	PO	no	D	11.06	11.70
	PON03	1	0.32	9.5	20	PO	no	D	5.40	6.41
	POS01	1	0.32	10	11.7	Ap	no	B	4.16	4.63
				15.3	20	PO	no	D	0.51	0.66
	POS02	1	0.32	9	20	PO	no	D	7.77	8.30
	POS03	1	0.32	1.5	5.5	Ap	no	B	10.37	20.51
				15.6	20	Po	no	D	0.86	0.90

* Sites in Figures 2 and 6; ls = lateral spreading; ma = marginal sand-blow; mo = moderate sand-blow

used; for the sites of type C and D it was chosen to use the coefficients calibrated for Ticino sand, which has grading and mineralogical composition similar to the Po river sand in the area of interest. The q_c values measured in the sandy layers with limited fine content where normalized according to Equation 4 and a CRR_5^{SS} profile was derived from q_c* using Equation 6. Figure 6 shows, for the same CPTs reported in Figure 2, the computed CRR_5^{SS} profiles (CRR PS, present study) and the cyclic earthquake-induced stress ratio profile CSR, which, according to Seed and Idriss (1971), was evaluated as follows:

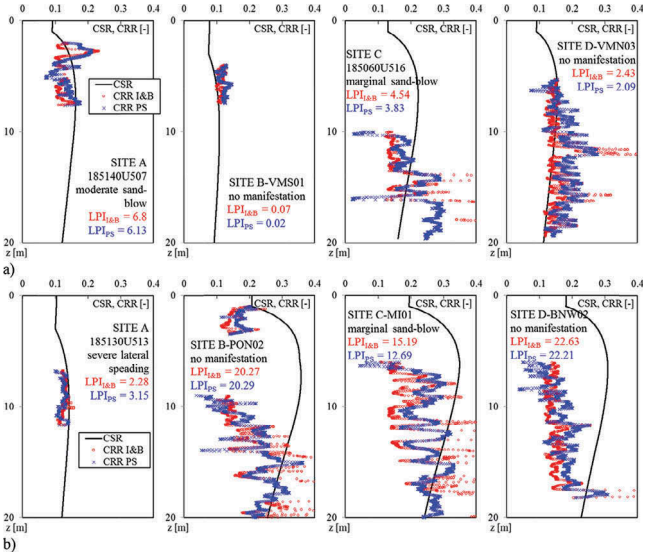

Figure 6. Example of liquefaction assessment results (a) prediction correct and (b) prediction failed.

$$\mathrm{CSR(z)} = 0.65(\sigma_v/\sigma'_v).(a_{max}/g).r_d(z) \tag{7}$$

where a_{max} is maximum ground surface acceleration reported in Table 3 and r_d is the shear stress reduction coefficient, computed as suggested by Idriss (1999). For comparison, the CRR profiles computed according to Boulanger and Idriss (2014) (CRR I&B) are also reported. In the sites of Figure 6a the prediction of the liquefaction assessment is consistent with the observations; in the sites of Figure 6b the prediction failed. The liquefaction potential index LPI values, computed according to Iwasaki et al. (1982) using the two methods compared in this paper, are listed in Table 3. The following consideration can be made:

- The method presented in this study is in general good agreement with the Boulanger and Idriss (2014) method and the factor of safety against liquefaction computed with the two methods are comparable;
- The LPI computed for sites of type A (i.e. at San Carlo and Mirabello) is lower than 5 (threshold LPI value for no surficial manifestation according to the Iwasaki criterion) in 17 out of 18 cases in contrast with the severity of the liquefaction manifestation observed; in the 17 cases LPI is lower than 3; however, the factor of safety against liquefaction resulted lower than one in the layer which liquefied during the 20 May 2012 earthquake;
- This suggests that, as also observed by Maurer et al. (2015), the damage potential of lateral spreading may not be well estimated by LPI;
- In the sites of type B, the factor of safety FS is underestimated in 3 out of 4 cases;
- In the sites of C type, the prediction in terms of FS is consistent with the field manifestations only in one case;
- In sites of type D, the prediction in terms of FS is inconsistent with the field observation in 7 cases;
- Excluding sites of type A (i.e. excluding lateral spreading manifestations), the liquefaction hazard prediction is overestimated in 50% of cases.

4 FINAL REMARKS

The method presented in this paper gives comparable result as the Boulanger and Idriss (2014) liquefaction evaluation procedure, as can be seen in Figure 6, where the CRR profiles computed with both methods are reported.

The liquefaction potential index LPI (Iwasaki criterion) under-predicted the liquefaction occurrence in all the sites where lateral spreading happened. As previously observed by Youd et al. (2002), Maurer et al. 2015, other criteria than LPI should be used for assessing lateral spreading manifestations. The methods adopted to assess liquefaction hazard in the test sites produced 50% wrong predictions (Table 3). As shown by Upadhyaya et al. 2018, a possible reason of wrong prediction is the presence of interbedded plastic soils suppressing liquefaction manifestation typical of alluvial sandy deposits as those investigated in this study. Moreover, a crucial effect can be the sandy soils degree of saturation. As shown in Figure 1 and detailed in Table 3, sandy deposits of similar origin and age to that present at San Carlo did not liquefied in areas closer to the 2012.05.20 and 2012.05.29 earthquake epicentres, where very high PGAs were measured (or estimated), suggesting the possibility of partial saturation of those soils. This hypothesis is supported by frequent reporting of gas leaks from the soil and presence of gas in the ground water just in the area few kilometres around the earthquake epicentre.

REFERENCES

Been, K. & Jefferies, M.G. 1985. A state parameter for sands. Géotechnique, 35(2), 99–112.

Boulanger & Idriss 2014. CPT and SPT based liquefaction triggering procedures. Report NO. UCD/CGM-14/01, Center For Geotechnical Modeling. Department of Civil & Environmental Engineering College of Engineering University of California at Davis.

Fioravante, V., Giretti, D., Abate, G., Aversa, S., Boldini, D., Capilleri, P.P., Cavallaro, A., Chamlagain, D., Crespellani, T., Dezi, F., Facciorusso, J., Ghinelli, A., Grasso, S., Lanzo, G., Madiai, C., Massimino, M.R., Maugeri, M., Pagliaroli, A., Rainieri, C., Tropeano, G., Santucci De Magistris, F., Sica, S., Silvestri, F., Vannucchi, G. 2013. Earthquake geotechnical engineering aspects of the 2012 Emilia-Romagna earthquake (Italy). In: 7th International conference on case histories in geotechnical engineering, April 29–May 4, 2013, Chicago

Fioravante V & Giretti D 2016. Unidirectional cyclic resistance of Ticino and Toyoura sands from centrifuge cone penetration tests. Acta Geotechnica, 11(4), 953–968.

Giretti, D. & Fioravante, F. 2017. A correlation to evaluate cyclic resistance from CPT applied to a case history. Bulletin of Earthquake Engineering, 15(5), 1965–1989.

Idriss, I.M. 1999. An update to the Seed–Idriss simplified procedure for evaluating liquefaction potential. Proc., Workshop New Approaches to Liquefaction Analysis, Federal Highway Administration, Washington, DC.

Ishihara, K., Iwamoto, S., Yasuda, S. & Takatsu, H. 1977. Liquefaction of anisotropically consolidated sand. Proceedings 9th International Conference on Soil Mechanics and Foundation Engineering, Japanese Society of Soil Mechanics and Foundation Engineering, Tokyo, Japan, Vol. 2, pp 261–64.

Ishihara, K., Yamazaki, A., & Haga, K. 1985. Liquefaction of K0 consolidated sand under cyclic rotation of principal stress direction with lateral constraint, Soils and Foundations, 5(4): 63–74.

Iwasaki T, Tokida K, Tatsuoka F, Watanabe S, Yasuda S, Sato H 1982. Microzonation for soil liquefaction potential using simplified methods. Proceedings of the 3rd International Conference on Microzonation, Seattle, vol 3, 1319–1330

Jaky, J. 1944. The coefficient of earth pressure at rest. Journal of the Society of Hungarian Architects and Engineers, Budapest, pp 355–358.

Li, X.S. & Wang, Z.L. 1998. Linear representation of steady state line for sand. J. Geotech. Geoenviron. Eng., ASCE, 124(12), 1215–1217.

Maurer, B. W., Green, R.A., Cubrinowski, M. & Bradley, B.A. 2015. Assessment of CPT-based methods for liquefaction evaluation in a liquefaction potential index framework. Geotechnique 65(5), 328–336.

Seed, H.B. & Idriss, I.M. 1971. Simplified procedure for evaluating soil liquefaction potential. J. Soil Mech. Found. Div., 97(9): 1249–1273.

Upadhyaya, S., Maurer, B.W., Grenn, R.A. & Rodriguez-Mareq, A. 2018. Effect of Non-Liquefiable High Fines-Content, High Plasticity Soils on Liquefaction Potential Index (LPI) Performance. Geotechnical Earthquake Engineering and Soil Dynamics V, June 10–13, 2018 | Austin, Texas.

Youd, T. L., Hansen, C. M. & Bartlett, S. F. 2002. Revised multilinear regression equations for prediction of lateral spread displacement. J. Geotech. Geoenviron. Engng 128(12) 1007–1017.